Measurement 234 (2024) 114926

Contents lists available at ScienceDirect

Measurement

journal homepage: www.elsevier.com/locate/measurement

Quantitative digital image correlation approach for the monitoring of fatigue damage development in 10CrMo9-10 steel in the as-received state and after extended service

Mateusz Kopec [a,*], Adam Brodecki [a], Zbigniew L. Kowalewski [a]

[a] Institute of Fundamental Technological Research, Polish Academy of Sciences, 5b Pawińskiego Str., 02-106 Warsaw, Poland

ARTICLE INFO

Keywords:
Power engineering steel
Fatigue
Damage
Digital image correlation (DIC)

ABSTRACT

In this paper, the quantitative Digital Image Correlation (DIC) approach was used to study the long-time degradation of two different states of 10CrMo9-10 (10H2M) power engineering steel. The specimens subjected to cyclic loading (R = 0) were monitored by using the DIC technique. The data obtained from DIC measurements were presented in form of strain distributions for specified, independent points within the strain gauge of specimens. Furthermore, the strain profiles were extracted for the particular stages of fatigue damage development (FDD). The presented methodology provides a different approach of DIC application, in which, the data could be treated more quantitative than qualitative.

1. Introduction

Comparative analysis of materials in their as-received states and after extended service is the commonly used approach for evaluating the mechanical behaviour of materials after long-term operation. The traditional techniques employed to compare and evaluate the mechanical responses of different material states involve extensometer and tensometer measurements. It is important to note, however, that these methods provide an average data from specified specimens area, since they can only monitor a limited strain gauge [4]. This limitation significantly hinders accurate predictions of crack localization during testing, as fatigue damage initiation is strongly localized. To address this issue, full-field optical methods can be utilized. They are offering several advantages such as the ability to measure fatigue crack closure and residual stress, as well as monitor stress concentration and stress gradients [2–4]. Among the optical methods, DIC is known as a convenient and effective tool for strain measurements. Niendorf et al. [5] confirmed the effectiveness of the DIC technique in monitoring of the damage evolution due to fatigue in ultrafine-grained steel subjected to low-cycle fatigue (LCF). The research findings indicated, that DIC successfully identified the region where cracks began to form at the beginning of cyclic deformation by capturing the accumulated high strain, which then built up and eventually resulted in the development of surface cracks. Qvale et al. [6] introduced a DIC-based method that proves to be highly efficient in detecting potential areas of fatigue crack initiation areas on the corroded surface. The reported approach enabled the precise detection of numerous crack initiation regions on the investigated surface. Risbet et al. [7] employed the DIC method to detect early damage in stainless steel operated under LCF conditions. This approach was utilized to develop a material model capable of accurately predicting the fatigue lifetime of structural components. El Bartali et al. [8] introduced an effective DIC-based method for conducting measurements during LCF to reveal the FDD mechanisms of X2CrNiMo25-07 austenitic-ferritic stainless steel. Their findings highlighted the significance of strain field measurements as a valuable tool for investigating the behaviour of metals experiencing fatigue damage, particularly in relation to strain gradients that serve as early indicators of microcrack formation. Koster et al. [9] used DIC to analyze the distribution of strain in brazed specimens produced from the steel X3CrNiMo13-4 steel as base material and with AuNi18 as a filler metal. The researchers emphasized the need for additional experiments that combine DIC and conventional extensometer recordings to accurately quantify the strain accumulation caused by cyclic loading and gain deeper insights into the mechanisms of failure. Kopec [10] presented a successful DIC approach in which selected strain profiles registered for the 13HMF steel specimens subjected to fatigue testing at stress amplitude equal to 380 MPa and 500 MPa were distinguished. It was concluded, that such representation could serve as an effective indicator of damage development because the

* Corresponding author.
E-mail address: mkopec@ippt.pan.pl (M. Kopec).

https://doi.org/10.1016/j.measurement.2024.114926
Received 13 March 2024; Received in revised form 30 April 2024; Accepted 15 May 2024
Available online 17 May 2024

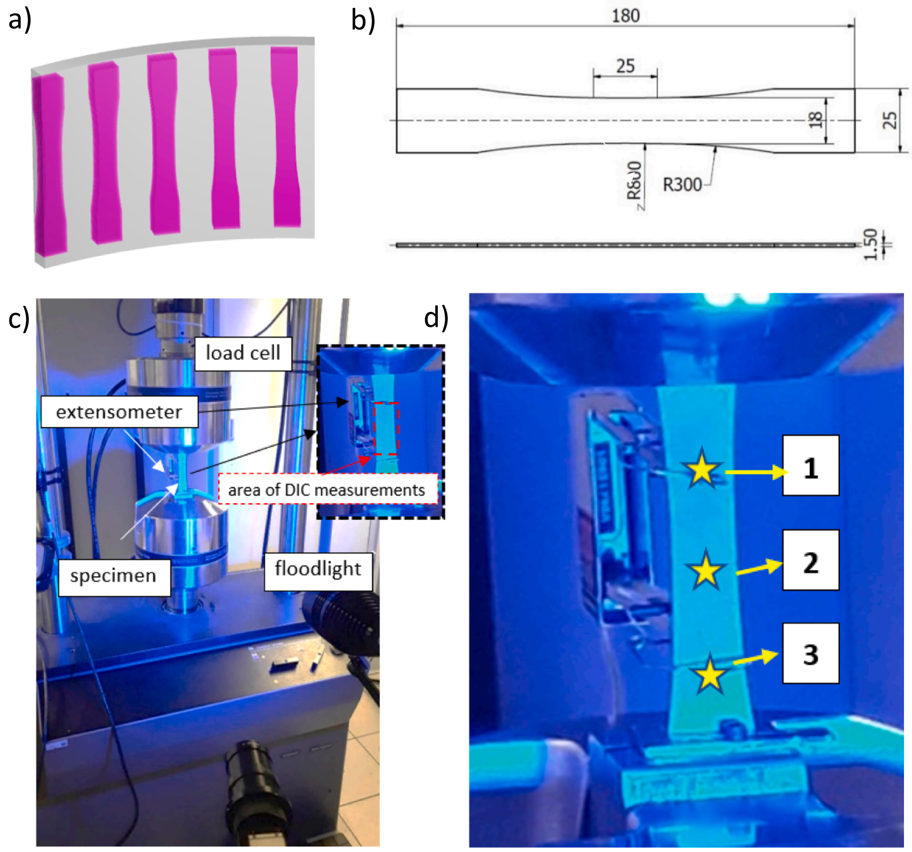

Fig. 1. Schematics of specimens distribution in a pipe (a); the geometry of the specimen (b); experimental setup (c); referring points used in quantitative DIC measurements (d).

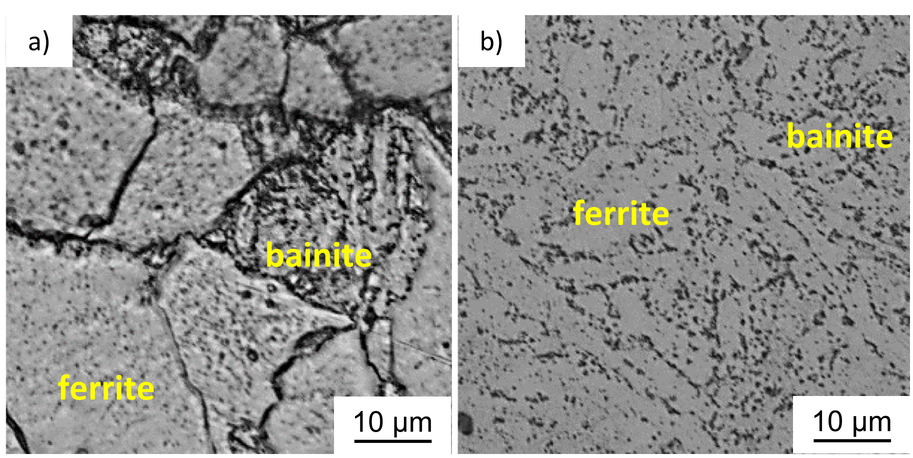

Fig. 2. The micrographs of 10H2M steel in the as-received state (a) and after extended service (b).

deformation on the specimen surface registered for a particular fatigue cycle indicates the process dynamics. The recent review on the application of DIC in fatigue experimentation by Hebert and Khonsari [11] highlights, that DIC provides more information than extensometer. Full-field strain distribution derived from DIC can be collected from macro and micro to nanoscale and can be correlated with microstructural characteristics, interacting surfaces, and fatigue crack nucleation and subsequent propagation. Such features only confirm that the DIC technique will remain a key tool for ongoing and upcoming studies on fatigue. It has to be emphasized, that many analyses involving mechanical testing supported by DIC are employing strain distribution maps as the research final outcome. However, this approach is usually providing qualitative data.

Considering the indisputable benefits of the DIC application in FDD monitoring, the primary objective of this study was to evaluate the impact of 280 000 h of service on the mechanical properties of 10CrMo9-10 steel through a DIC-based quantitative approach.

2. Materials and methods

The wire-cut specimens were extracted from 10CrMo9-10 steel pipes delivered in both, the as-received state and after prolonged service for 280 000 h at a temperature equal to 540 °C and an internal pressure of 2.9 MPa. Fig. 1a-b displays the specimen distribution in a pipe and their

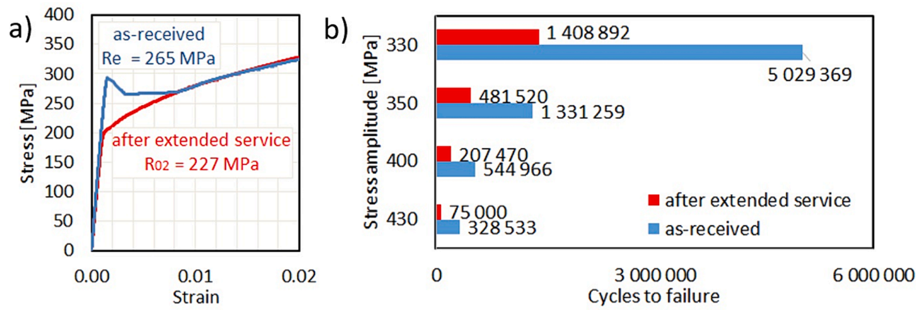

Fig. 3. Determination of the yield point for 10CrMo9-10 steel in both states (a); service life of 10CrMo9-10 steel subjected to different stress amplitudes (b).

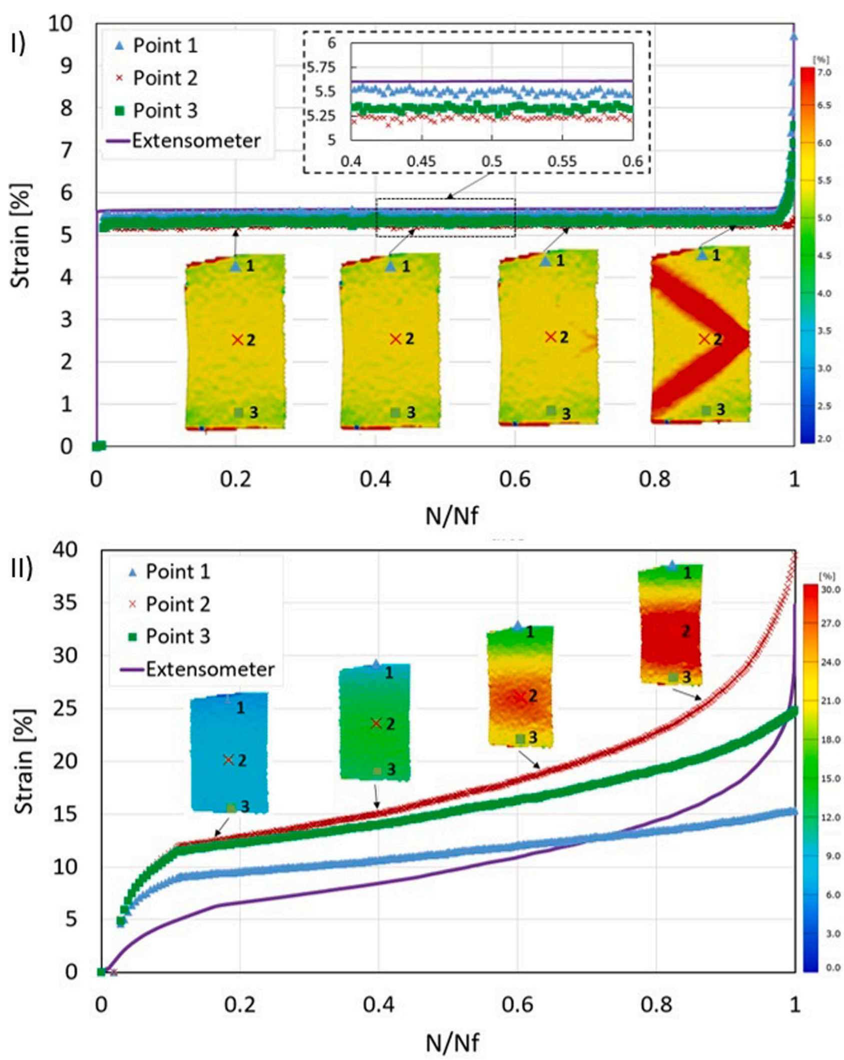

Fig. 4a. Comparison of strain evolution registered by DIC in three independent points with extensometer recordings for the steel in as-received state (I) and after extended service (II) under stress amplitude of 430 MPa.

geometry, respectively. Initially, uniaxial tensile tests were conducted at a strain rate of 0.0002 s^{-1} to determine the properties of the 10CrMo9-10 steel in both states. Subsequently, fatigue loading conditions were established on the basis of the yield strength $R_{0.2}$ value. Uniaxial tensile tests as well as fatigue were conducted using the MTS 858. The fatigue tests were performed at a frequency of 20 Hz under stress control, stress asymmetry ratio R = 0, a mean stress level of (σ_{max}- σ_{min})/2, and stress amplitudes equal to 330 MPa, 350 MPa, 400 MPa and 430 MPa. The measurement of strain evolution was conducted utilizing the standard MTS extensometer with a gauge length equal to 25 mm. The fatigue tests were also assisted by DIC Aramis 12 M, which was calibrated using GOM calibration plate for a measuring area of 170x156 mm. An overview of the experimental setup can be seen in Fig. 1c while referring points used in quantitative DIC data analysis were shown in Fig. 1d. The Aramis software allowed for the automatic capturing of DIC images at the maximum value of stress in each cycle and after every thousand fatigue cycles.

In the final step of the experimental programme, the data obtained

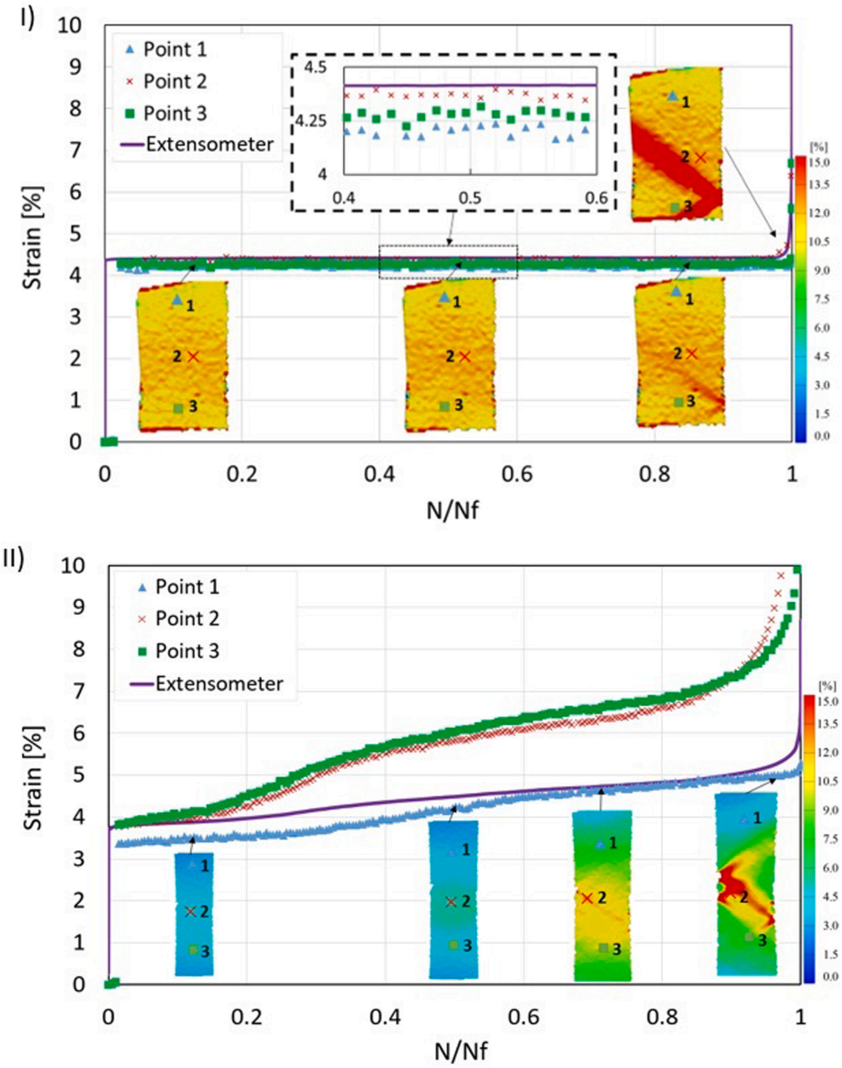

Fig. 4b. Comparison of strain evolution registered by DIC in three independent points with extensometer recordings for the steel in as-received state (I) and after extended service (II) under stress amplitude of 400 MPa.

from the extensometer as well as from DIC was compared and further used for a quantitative assessment of FDD based on deformation changes registered on the specimen surface. During the data analysis, three different points were used as the reference (Fig. 1d). Points 1 and 3 were arranged to be relatively close to the legs of the extensometer fixed to the specimen, whereas point 2 was set in the geometrical centre of the specimen. For each of the marked points, strain values were extracted for a specific fatigue cycle. Subsequently, they were related to the absolute value N/Nf, which is the quotient of the cycle divided by the total number of cycles to failure.

3. Results

The microstructure examination showed that the extended service caused a significant changes in the phase composition of the 10H2M steel. Initially, the ferritic-bainitic microstructure, consisting of lath or plate-shaped ferrite packets (Fig. 2a), was transformed into a structure of bainite-ferrite with carbides formed at the grain boundaries (Fig. 2b). One should mention, that during degradation of the 10H2M steel, a significant phase transformations occur, resulting in the growth of ferrite laths and formation of the equiaxed ferrite grain structure. Moreover, the excessive transformation of M_2X carbides into $M_{23}C_6$/M_6C, and their subsequent precipitation along the boundaries of the ferrite grains substantially decrease the mechanical behaviour of 10H2M steel.

Yield strength values for both states of 10CrMo9-10 steel were obtained from the uniaxial tensile tests (Fig. 3a). The material after prolonged service exhibited a notably lower value of the yield strength. Such a fact provides important information about the effect of extended service already at such a stage of the experiment. Subsequent fatigue tests executed on both states of materials exposed significant differences in service lifetime, as illustrated in Fig. 3b. Specifically, the material after extended service was only able to endure half the number of cycles compared to its as-received condition when subjected to testing at the same stress amplitude. A notable decrease up to 400 % was observed for such state of material. It was reported, that prolonged service duration results in a significant reduction of the fatigue lifetime of pipes, mainly due to the defects concentration in the material over time [12].

The analysis of data captured by DIC for 10CrMo9-10 steel in both states of the material enables to determine the dynamics of FDD. It was observed, that the material after service exhibited strain increase in subsequent fatigue cycles when subjected to stress amplitude of 430 MPa. On the other hand, the as-received one, after reaching a strain level of approximately 5.5 %, showed practically no changes until the specimen failure (Fig. 4a). Similar material behaviour was observed for the stress amplitude equal to 400 MPa (Fig. 4b). The application of lower

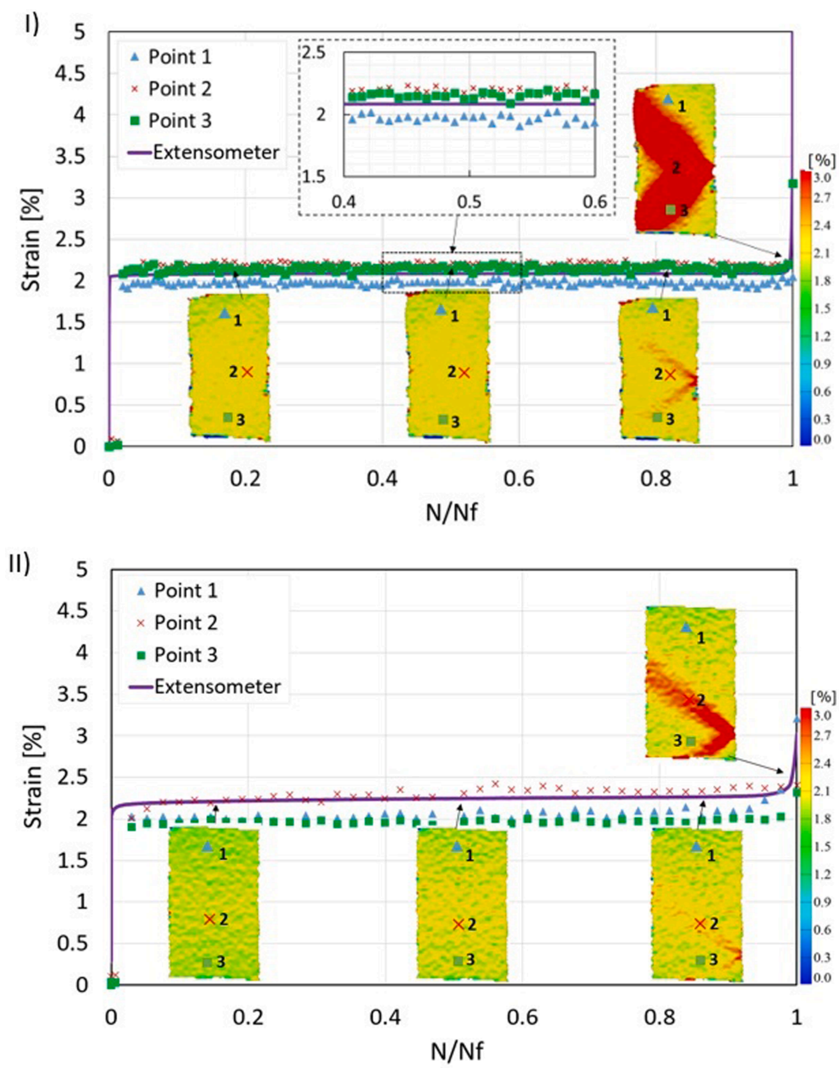

Fig. 4c. Comparison of strain evolution registered by DIC in three independent points with extensometer recordings for the steel in as-received state (I) and after extended service (II) under stress amplitude of 350 MPa.

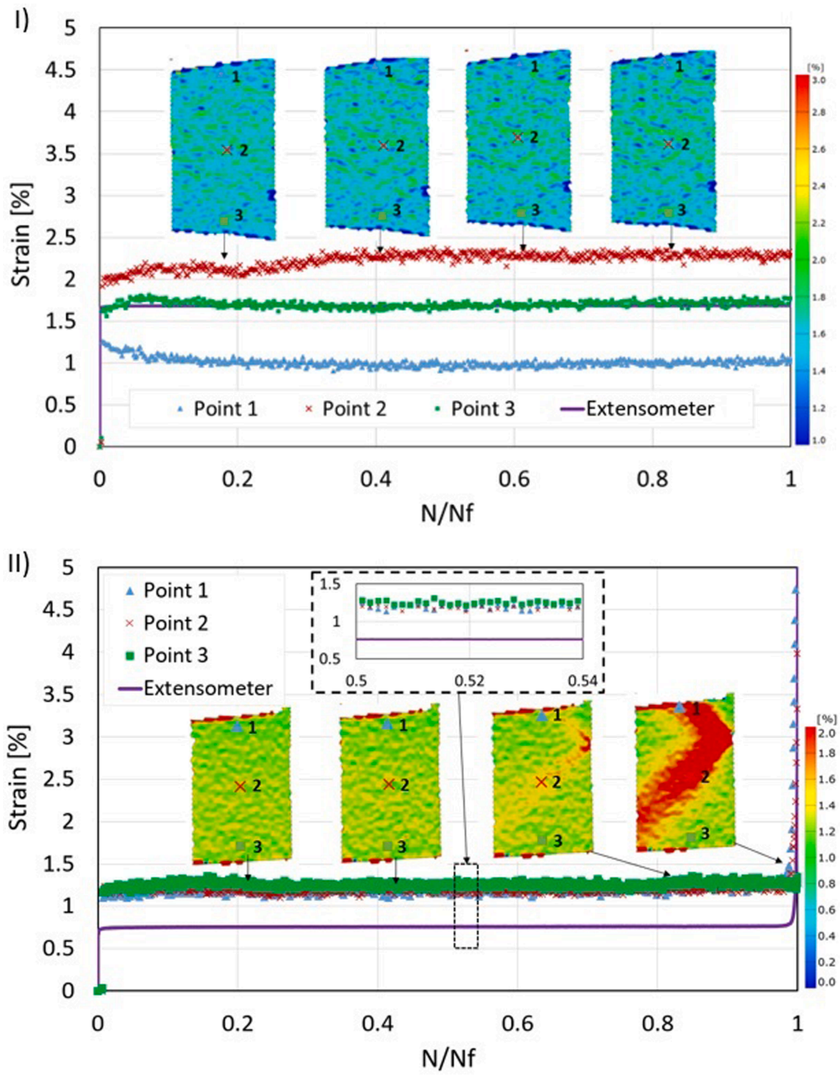

Fig. 4d. Comparison of strain evolution registered by DIC in three independent points with extensometer recordings for the steel in as-received state (I) and after extended service (II) under stress amplitude of 330 MPa.

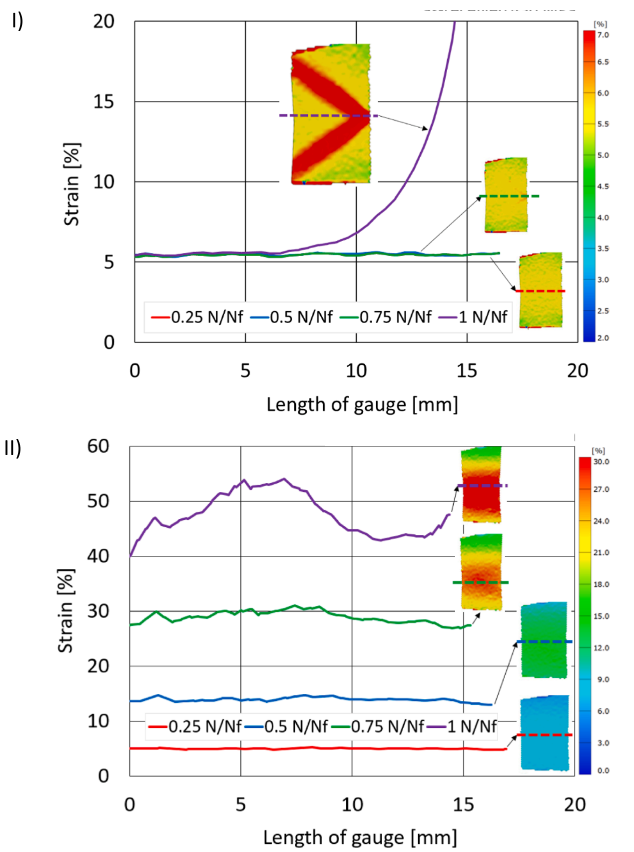

Fig. 5a. Strain profiles registered by DIC during fatigue tests for the steel in as-received state (I) and after extended service (II) tested under stress amplitude of 430 MPa.

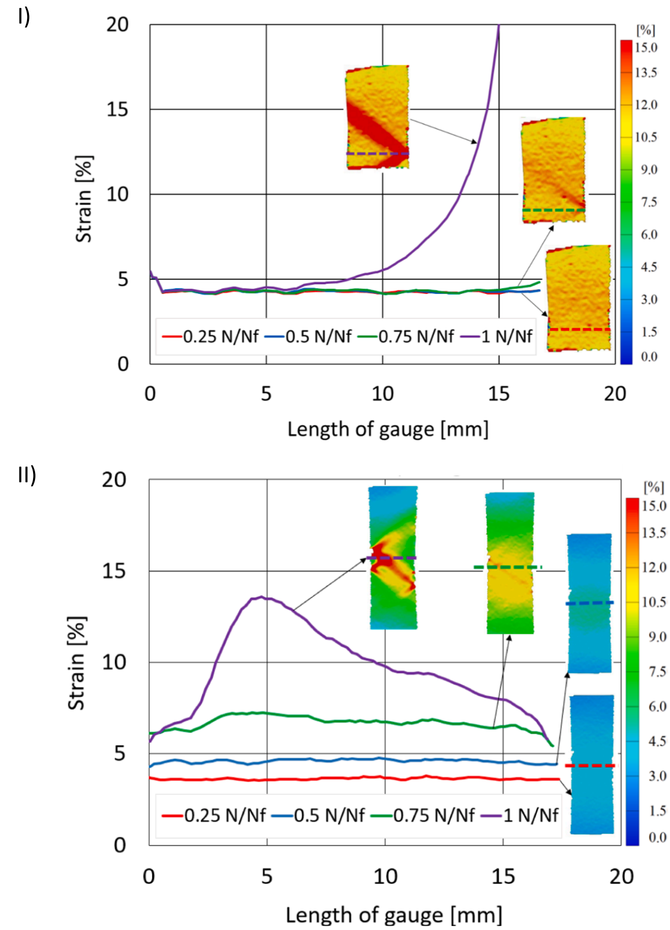

Fig. 5b. Strain profiles registered by DIC during fatigue tests for the steel in as-received state (I) and after extended service (II) tested under stress amplitude 400 MPa.

stress amplitude values of 330 MPa and 350 MPa resulted in similar characteristics of strain changes in relation to the total number of cycles to failure. Materials in both states, after reaching a constant strain offset kept a similar level of deformation until the fracture (Figs. 4c-d).

One should emphasize, how significantly the deformation patterns differ depending on the reference point selection. It was expected, that the strain recordings obtained from the extensometer should fall between the results from points 1 and 3 and point 2, which is the extreme value of strain resulting from the accumulation of strain in the area of the specimens neck. However, the experimental results differ locally from the expected ones. This is mainly due to the location of points 1 and 3 near the extensometer legs.

In case of the as-received material tested under the stress amplitude equal to 430 MPa, point 2 localized in the centre of the gauge was outside the area of the greatest strain accumulation (Fig. 4a(I)). Therefore, the strain values registered for this point were lower than those captured for point 3. It is worth noting that for such a case, point 1 was located in the borderline area, where dark red zone was observed in the upper left corner of the strain distribution map. Theoretically, this area should correspond to a place of high deformation, which, however, does not reflect the actual condition of the material. Similar behaviour was observed for the material after long-term usage subjected to a stress amplitude equal to either 430 MPa (Fig. 4a(II)) or 400 MPa (Fig. 4b(II)), where an increase in the strain level was recorded at point 3. For both values of stress amplitude, the average strain value recorded by the extensometer for the as-received material was higher than that for the separately registered strain evolutions. However, a high strain increase accumulating in the central part of the specimen (Fig. 4a(II)) or the initiation of crack in more than one area (Fig. 4b(II)) may indicate high heterogeneity of the material after long-term use. The effectiveness of the proposed methodology for monitoring an evolution of strain, is more pronounced when lower stress amplitude values (350 MPa and 330 MPa) are applied (Figs. 4c-d). Regardless of the amplitude and material state, the strain accumulation is observed in the central part of specimen (point 2).

On the other hand, the analysis of strain profiles in any selected line on the specimen surface is undoubtedly an useful tool in the analysis of strain distribution during fatigue tests (Figs. 5a-d). Since the colour distribution on the specimen surface provides only qualitative information about damage development, examination of a strain profile in a given section provide quantitative results, that enable to predict favoured areas and directions of potential crack initiation and its subsequent development. Execution of comparative tests on both states of steel could be also helpful in determination of the damage development dynamics in relation to the entire course of the fatigue test. Using as an example the stress amplitude of 430 MPa, a significant increase of strain oscillations was observed along the given cross-section, located 5 mm from the edge of specimen (Fig. 5a (II)). It is worth emphasizing, that in the strain distribution map only red colour, suggesting an essential strain accumulation, is visible. During the strain profile analysis through the accumulation area, significant strain variations of almost 15 % were observed. Additionally, the highest strain was also located 5 mm from the specimen edge for the test under stress amplitude of 400 MPa (Fig. 5b (II)). Such behaviour indicates, that for a high stress amplitude, strain accumulates inside the material, not at the edge of the specimen. The opposite effect can be observed for low stress amplitude values, where for 350 MPa and 330 MPa, a strongly localized strain was observed on the specimen edges.

Finally, data generated from DIC measurements executed during

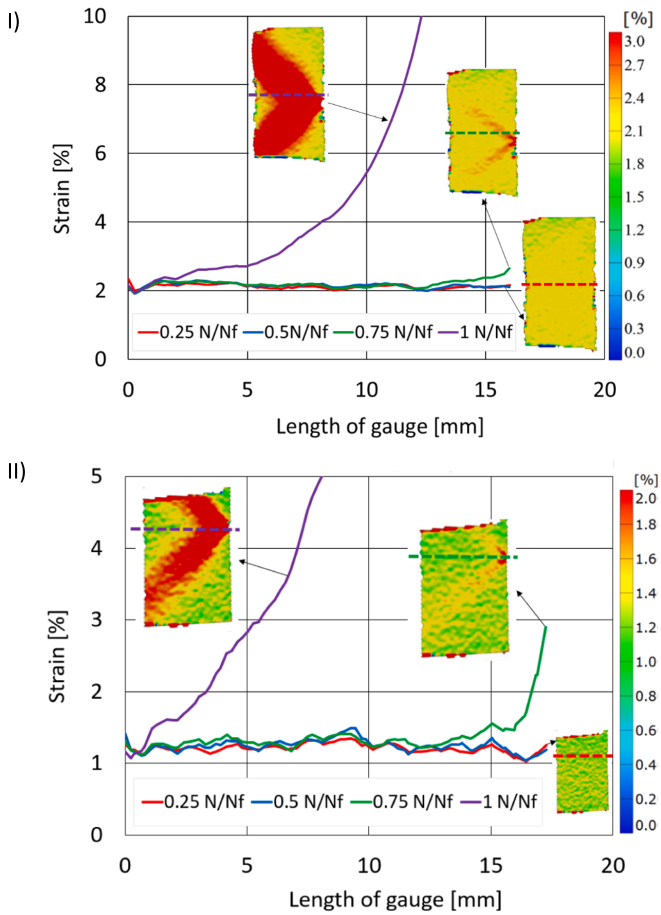

Fig. 5c. Strain profiles registered by DIC during fatigue tests for the steel in as-received state (I) and after extended service (II) tested under stress amplitude of 350 MPa.

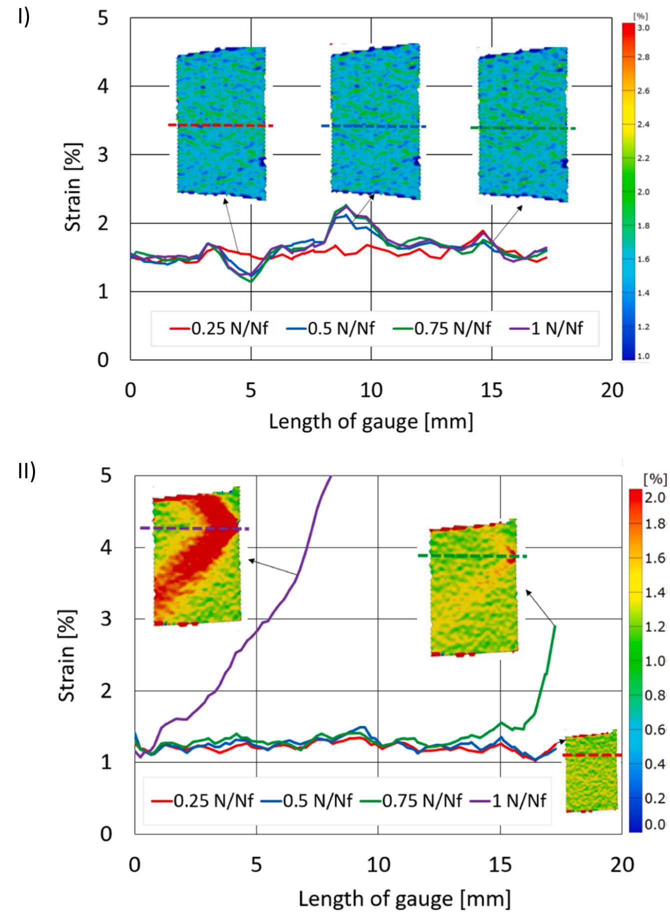

Fig. 5d. Strain profiles registered by DIC during fatigue tests for the steel in as-received state (I) and after extended service (II) tested under stress amplitude of 330 MPa.

fatigue tests was used to visualise strain distribution for the as-received (blue colour) material and after extended service (red colour) tested under different stress amplitudes (Fig. 6). Such data was presented in the form of a cloud of points for the entire test, till specimen fracture. The relatively flat character of the cloud for the as-received material was associated with the similar strain behaviour observed in Figs. 4a-d (I). Once the material reached a certain strain level, its value was stable till the specimen fracture. On the other hand, an unstable increase of strain with the subsequent number of cycles to failure was observed for material after prolonged service. Such behaviour was more prominent with the increase of the stress amplitude above 400 MPa. One should mention, that at the beginning of the test, the material after extended service already reached the strain value equal to 4 % and with subsequent cycles, such strain increased rapidly up to specimen fracture. Such differences are negligible at stress amplitudes of 330 MPa and 350 MPa, for which the data overlapping could be observed (Fig. 6). Based on such results, it was concluded, that the importance of long-time degradation assessment for 10CrMo9-10 steel under pulsating loading is extremely important in low cycle fatigue regime. The uncontrolled increase of strain, resulting from the degraded microstructure (Fig. 2), accelerates the FDD thus significantly reducing its service.

Among several advantages of the DIC system, one can distinguish the contactless, full-field, and multipoint measurements, ensuring high efficiency and measurement accuracy and stability. It offers high precision over the entire area and a wide measurement range, from several millimetres to meters, even at high temperatures. Additionally, it provides an accurate measurements of structures in typical outdoor environments, enabling full-field deformation analysis. The quick preparation of

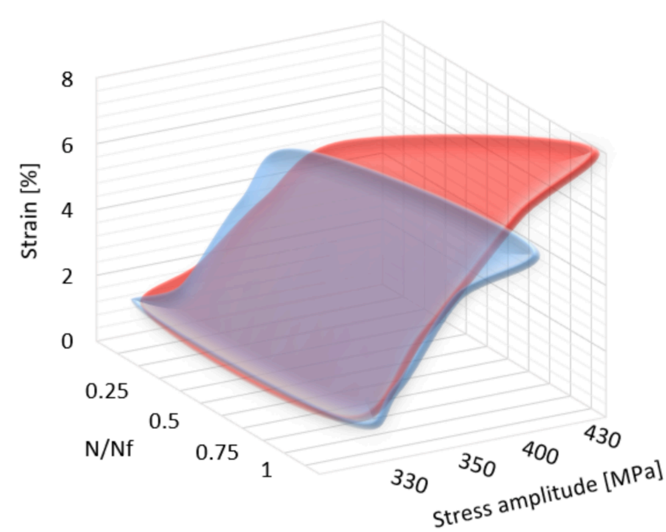

Fig. 6. Strain distribution cloud data generated from DIC measurements executed during fatigue tests for the as-received (blue colour) material and after extended service (red colour) tested under different stress amplitudes.

a random pattern of black dots on the white background on the specimen surface by spraying paint is essential for this process. Despite its many advantages, some limitations. The specimen surface must be planar with a random pattern, and artificial light may be necessary when registering images with high frequency. Calibration A special calibration tables appropriate to the size of the tested specimen area are required, along with the capacious storage media to archive the recorded images. Measurement errors are strongly dependent on a size of the measuring area. Therefore, a resolution, image noise and other inaccuracies resulting from changes in light conditions during testing, noises from the digital camera, an angle between cameras and the surface analysed, and the lenses quality may affect the results of calculations [1].

4. Conclusions

The proposed methodology for the strain distribution analysis using DIC could be used to effectively assess an effect of long-term degradation on the mechanical response of materials. Comparison of the strain distribution for three reference points and the average value captured by the extensometer, together with the analysis of strain profile along the specimens width for various stages of damage development recorded during fatigue test enables the following conclusions to be formulated:

- application of a high stress amplitude (400 MPa and 430 MPa) for the material after extended service leads to the accumulation of strain in the central part of specimen. An initiation of the crack site is difficult to predict, as it occurs at the final stages of specimens life, indicating a high heterogeneity of the material. In turn, the material in the as-received state, after reaching a stable strain level, maintains its constant level until a crack is initiated due to the localization of the strain on the specimen edge.
- adoption of the lower stress amplitude values equal to 330 MPa and 350 MPa, regardless of the material state, results in stable damage development, however, the prediction of the expected crack initiation area is only possible for the material in its as-received condition. After long-term service, the material is susceptible to crack initiation that is difficult-to-predict in the final stages of fatigue.

CRediT authorship contribution statement

Mateusz Kopec: Writing – review & editing, Writing – original draft, Visualization, Validation, Supervision, Methodology, Investigation, Formal analysis, Data curation, Conceptualization. **Adam Brodecki:** Visualization, Methodology, Investigation, Data curation. **Zbigniew L. Kowalewski:** Writing – review & editing, Validation, Supervision, Project administration, Methodology, Conceptualization.

Declaration of competing interest

The authors declare that they have no known competing financial interests or personal relationships that could have appeared to influence the work reported in this paper.

Data availability

Data will be made available on request.

Acknowledgements

The authors would like to express their gratitude to the technical staff – Mr M. Wyszkowski for his kind help during the experimental part of this work.

This work has been partially supported by the National Science Centre through Grant No 2019/35/B/ST8/03151.

References

[1] M. Kopec, A. Brodecki, D. Kukla, Z.L. Kowalewski, Suitability of DIC and ESPI optical methods for monitoring fatigue damage development in X10CrMoVNb9-1 power engineering steel, Archiv. Civ. Mech. Eng 21 (2021) 167, https://doi.org/10.1007/s43452-021-00316-1.

[2] D. Nowell, R.J.H. Paynter, P.F.P. De Matos, Optical methods for measurement of fatigue crack closure: moiré interferometry and digital image correlation, Fatigue Fract. Eng. Mater. Struct. 33 (2010) 778–790, https://doi.org/10.1111/j.1460-2695.2010.01447.x.

[3] D.V. Nelson, Residual stress determination using full-field optical methods, J. Phys. Photonics 3 (2021) 044003, https://doi.org/10.1088/2515-7647/ac1ceb.

[4] S. Sieberer, E.G. Viehböck, M. Schagerl, Optical stress concentration and stress gradient monitoring during elasto-plastic fatigue tests with Digital Image Correlation, Mater. Today: Proceedings 62 (2022) 2543–2548, https://doi.org/10.1016/j.matpr.2022.03.347.

[5] T. Niendorf, J. Dadda, D. Canadinc, H.J. Maier, I. Karaman, Monitoring the fatigue-induced damage evolution in ultrafine-grained interstitial-free steel utilizing digital image correlation, Mater. Sci. Eng. A 517 (2009) 225–234, https://doi.org/10.1016/j.msea.2009.04.053.

[6] P. Qvale, E.P. Zarandi, S.K. Ås, B.H. Skallerud, Digital image correlation for continuous mapping of fatigue crack initiation sites on corroded surface from offshore mooring chain, Int. J. Fatigue 151 (2021) 106350, https://doi.org/10.1016/j.ijfatigue.2021.106350.

[7] M. Risbet, P. Feissel, T. Roland, D. Brancherie, J.M. Roelandt, Digital Image Correlation technique: application to early fatigue damage detection in stainless steel, Procedia Eng. 2 (2010) 2219–2227, https://doi.org/10.1016/j.proeng.2010.03.238.

[8] A. El Bartali, V. Aubin, S. Degallaix, Fatigue damage analysis in a duplex stainless steel by digital image correlation technique, Fatigue Fract. Eng. Mater. Struct. 3 (2008) 137–151, https://doi.org/10.1111/j.1460-2695.2007.01207.x.

[9] M. Koster, C. Kenel, W.J. Lee, C. Leinenbach, Digital Image Correlation for the Characterization of Fatigue Damage Evolution in Brazed Steel Joints, Procedia Mater. Sci. 3 (2014) 1117–1122, https://doi.org/10.1016/j.mspro.2014.06.182.

[10] M., Kopec Fatigue damage development in 14MoV6-3 steel for powerplant pipes monitored by digital Image correlation, Acta Mechanica Solida Sinica 36 (2023) 405–417, https://doi.org/10.1007/s10338-023-00387-y.

[11] J. Hebert, M., Khonsari The application of digital image correlation (DIC) in fatigue experimentation: A review, Fatigue Fract. Eng. Mater. Struct. 46 (2022) 1256–1299, https://doi.org/10.1111/ffe.13931.

[12] S.V. Panin, I.V. Vlasov, P.O. Maruschak, A.V. Eremin, F. Berto, A. S. Syromyatnikova, A. Vinogradov, Influence of long-term cold climate operation on structure, fatigue durability and impact toughness of 09Mn2Si pipe steel, Eng. Fail. Anal. 102 (2019) 87–101, https://doi.org/10.1016/j.engfailanal.2019.04.036.